NONLINEAR OPTICALLY DETECTED ELECTROPHONON RESONANCE LINEWIDTH IN DOPED SEMICONDUCTOR SUPERLATTICES

HUYNH VINH PHUC, LUONG VAN TUNG
Dong Thap University, No. 783, Pham Huu Lau Str., Dong Thap
LE DINH, TRAN CONG PHONG[1]
Hue University's College of Education, No. 34, Le Loi Str., Hue City

Abstract. *In this paper, the analytic expression for nonlinear absorption power (NAP) in a doped semiconductor superlattice (DSSL) is obtained by using the operator projection technique in case of electron-optical phonon scattering. We have obtained nonlinear optically detected electrophonon resonance (NODEPR) condition as a function of well width and concentration of the donor impurities. Anomalous behaviors of the NODEPR spectrum such as the splitting of NODEPR peaks for two photon absorption process are discussed. From the graphs of the NAP, we obtain the NODEPR linewidth as profiles of curves. Computational results show that the NODEPR linewidth increases with temperature T, and with the donor impurities n_D, and decreases with the period d of a DSSL. The contribution of two-photon absorption process to absorption power is smaller than one of one photon process.*

I. INTRODUCTION

The linewidth, including ODEPR linewidth, is one of good tools for investigating scattering mechanisms of carriers. The vast majority of works on the linewidth has been done on the transport properties of semiconductors. To investigate the effects of various scattering processes, absorption linewidth have been measured in various kind of semiconductors, such as quantum wells [1, 2, 3, 4, 5], quantum wires [6, 7, 8, 9, 10], and quantum dots [11]. The linewidth has been studied both in theoretical works [1, 2, 3, 4, 5, 6, 7, 8, 9, 10] and in experimental works [11, 12]. Most of these results show that the linewidth increases with temperature and decreases with system's size.

The study of the electrophonon resonance (EPR) effects is very important in understanding transport phenomena in semiconductor, and hence the EPR phenomena in low-dimensional systems has generated considerable interest in the recent years in 3D semiconductor systems [13], in quantum wells [14, 15], in quantum wires [16, 17], and quantum dots [18]. These articles have demonstrated the the splitting of ODEPR peaks and appearance or disappearance of the EPR and ODEPR peaks due to the selection rules [15]. But the study of the ODEPR linewidth remains an open problem.

Recently, our group [19, 20] has developed the theory of Lee and co-works [21] on the nonlinear optical conductivity due to electron-phonon interacting in semiconductor in the presence of electromagnetic waves. In previous papers, we have obtained expression

---

[1]Present Address: National Education Union of Vietnam, 2 Trinh Hoai Duc, Dong Da, Ha Noi.

of nonlinear absorption power in which the two photon process is included, and have obtained nonlinear absorption linewidth in rectangular quantum wires [19] and in cylindrical quantum wires [20].

In this paper, we expand the results of one of our previous papers [20] to investigate the linear and nonlinear ODEPR linewidth in DSSL. The present work is fairly different in comparison to the previous results because the ODEPR effect is taken into account and the results can be applied to optically detect the resonant peaks. We know, the linewidth are defined by the profile of curves describing the dependence of absorption power $P(\omega)$ on the photon energy or frequency [22, 23]. Firstly, we obtain the analytical expression of linear and nonlinear absorption power in which the two photon process is included. Then, from the graph of the absorption power as a function of photon energy we obtain nonlinear ODEPR linewidth as a profiles of curves. The dependence of the nonlinear ODEPR linewidth on temperature T, the concentration of the donor impurities n_D, and period d of the DSSL is discussed. Finally, the results are compared to previous theoretical and experimental results.

II. NONLINEAR ABSORPTION POWER IN DSSL

The superlattice potential in DSSL is created solely by using the spatial distribution of the charge. A substantial improvement in spatial (on an atomic scale) monitoring of the doping during film growth by means of molecular-beam epitaxy enabled the growth of doped superlattices-periodic alternation of thin layers of GaAs of the n (GaAs:Si)-and p (GaAs:Be)-types, separated in many cases by layers of intrinsic GaAs. We consider a DSSL, in which the electron gas is confined by a superlattice potential along the z direction (the axis of the superlattice) and in which electrons are free on the $x-y$ plane. The motion of an electron is confined in each layer of the DSSL and its energy spectrum is quantized into discrete levels in the z direction. The electron state, $|\alpha\rangle$, is defined by the quantum number n in the z direction and the wave vector $\vec{k}_\perp$ on the $x-y$ plane perpendicular to z-axis, $|\alpha\rangle = |n, \vec{k}_\perp\rangle$, $\vec{k}^2 = k_\perp^2 + k_z^2$ [24].

In this paper, we will deal with bulk (3-dimensional) phonons; therefore, the electron-optical phonon interaction constant takes the forms [25]

$$|C_{\vec{q}}|^2 = \frac{e^2 \hbar \omega_{LO}}{2\epsilon_0 \Omega} \left(\frac{1}{\chi_\infty} - \frac{1}{\chi_0} \right) \frac{q_\perp^2}{(q_\perp^2 + q_d^2)^2}. \tag{1}$$

Here, e is the charge of electron, $\hbar \omega_{LO}$ is the energy of LO-phonon, ϵ_0 is the permittivity in vacuum, Ω is the volume of the system, χ_0 and χ_∞ are the static and the high frequency dielectric constants, respectively, and q_d is the reciprocal of the Debye screening length. The electron form factor, $M_{n,n'}(q_z)$, is given as [26]

$$M_{n,n'}(q_z) = \sum_{j=1}^{s_0} \int_0^d e^{iq_z z} \Phi_n(z - jd) \Phi_{n'}(z - jd) dz, \tag{2}$$

where d and s_0 are the period and the number of periods of the DSSL, respectively. $\Phi_n(z)$ is the eigenfunction of the electron in an individual potential well.

The energy spectrum of an electron in the DSSL for the state $|\alpha\rangle$ takes the form [27, 28, 29]

$$E_n(\vec{k}_\perp) = \frac{\hbar^2 k_\perp^2}{2m^*} + (n + 1/2)\hbar\omega_p = \frac{\hbar^2 k_\perp^2}{2m^*} + E_n, \tag{3}$$

with $\omega_p = (4\pi e^2 n_D/m^*\epsilon_0)^{1/2}$ is the plasma frequency. Here, m^* is the effective mass of the electron, n_D is the concentration of the donor impurities, and E_n are the energy levels of an individual well.

When an electromagnetic wave characterized by a time-dependent electric field of amplitude E_0 and angular frequency ω is applied, the absorption power $P(\omega)$ delivered to the system is given by $P(\omega) = (E_0^2/2)\text{Re}\{\sigma(\omega)\}$ [30, 31]. Here, $\sigma(\omega)$ is the optical conductivity tensor. Utilizing the general expression for the nonlinear conductivity that is presented by Lee *et al.* [21], the nonlinear absorption power at the subband edge ($k_\perp = 0$) in DSSL is given by the following set of expressions

$$\text{Re}\{\sigma_{NLn}(\omega)\} = \text{Re}\{\sigma_{zz}(\omega)\} + E_0\text{Re}\{\sigma_{zzz}(\omega)\}. \tag{4}$$

In Eq. (4), the first- and the second- term correspond to the linear and nonlinear terms of the conductivity tensor, given as follow, respectively.

$$\text{Re}\{\sigma_{zz}(\omega)\} = e \sum_{n,n'} |(z)_{n,n'}||(j_z)_{n,n'}| \frac{(f_{n',0} - f_{n,0})B_0(\omega)}{(\hbar\omega - \Delta E_{n',n})^2 + [B_0(\omega)]^2}, \tag{5}$$

$$\begin{aligned}
\text{Re}\{\sigma_{zzz}(\omega)\} = {} & e^2 \sum_{n,n',n''} \frac{|(z)_{n,n''}|(f_{n',0} - f_{n,0})}{(\hbar\omega - \Delta E_{n',n})^2 + [B_0(\omega)^2]} \\
& \times \left\{ \frac{|(z)_{n'',n}||(j_z)_{n',n''}|}{(2\hbar\omega - \Delta E_{n',n''})^2 + [B_1(\omega)^2]} \right. \\
& \times \; [(\hbar\omega - \Delta E_{n',n})B_1(\omega) + (2\hbar\omega - \Delta E_{n',n''})B_0(\omega)] \\
& + \frac{|(z)_{n',n''}||(j_z)_{n'',n}|}{(2\hbar\omega - \Delta E_{n'',n})^2 + [B_2(\omega)^2]} \\
& \times \; \left. [(\hbar\omega - \Delta E_{n',n})B_2(\omega) + (2\hbar\omega - \Delta E_{n'',n})B_0(\omega)] \right\},
\end{aligned} \tag{6}$$

where $\Delta E_{n',n} = E_{n'}(0) - E_n(0)$ with $E_n(0)$, $E_{n'}(0)$ and $E_{n''}(0)$ are the energy of the electron in the initial, final, and intermediate states, respectively; $f_{n,k_\perp}$ is the Fermi-Dirac distribution function of electron with energy $E_n(k_\perp)$; $|(z)_{n,n'}|$ and $|(j_z)_{n,n'}|$ are the matrix elements of the position- and current-operator, respectively. For calculating the nonlinear absorption power of electromagnetic wave in DSSL we use the following matrix elements

$$|(z)_{n,n'}| = |I_{n,n'}| = \left| \sum_{j=1}^{s_0} \int_0^d \Phi_n(z - jd)\Phi_{n'}(z - jd)z\,dz \right|, \tag{7}$$

$$|(j_z)_{n,n'}| = |J_{n,n'}| = \frac{e\hbar}{m^*} \left| \sum_{j=1}^{s_0} \int_0^d \Phi_n(z - jd)\frac{\partial}{\partial z}\Phi_{n'}(z - jd)\,dz \right|. \tag{8}$$

Here, we have used $j_z = (ie\hbar/m^*)\partial/\partial z$.

Quantity $B_0(\omega)$ in Eq. (5) is the imaginary part of damping function, $\Gamma_0^{\alpha\beta}(\bar\omega)$, which is given in Eq. (3.15) of Ref. [21]. The sum over $\vec{q}$ and intermediate state $|n",0\rangle$ are transformed into the integral, and realizing the calculations, we obtain

$$
\begin{aligned}
B_0(\omega) &= \frac{e^2\hbar\omega_{LO}}{2\epsilon_0(f_{n',0}-f_{n,0})}\frac{1}{2q_d^2} \\
&\times \sum_{n"}\Big\{|M_{n',n"}|^2\left[(1+N_q)f_{n",0}(1-f_{n,0})-N_qf_{n,0}(1-f_{n",0})\right]\delta(Y_{n,n"}^+) \\
&+ |M_{n',n"}|^2\left[N_qf_{n",0}(1-f_{n,0})-(1+N_q)f_{n,0}(1-f_{n",0})\right]\delta(Y_{n,n"}^-) \\
&+ |M_{n,n"}|^2\left[(1+N_q)f_{n',0}(1-f_{n",0})-N_qf_{n",0}(1-f_{n',0})\right]\delta(Y_{n',n"}^+) \\
&+ |M_{n,n"}|^2\left[N_qf_{n',0}(1-f_{n",0})-(1+N_q)f_{n",0}(1-f_{n',0})\right]\delta(Y_{n',n"}^-)\Big\},
\end{aligned}
\tag{9}
$$

where $n"$ is the quantum number of immediate states, respectively, and we have denoted

$$
Y_{n,n'}^{\pm} = \hbar\omega - (E_n - E_{n'}) \pm \hbar\omega_{LO}.
\tag{10}
$$

Quantities $B_1(\omega)$ and $B_2(\omega)$ in Eq. (6) are the imaginary part of nonlinear damping functions, which derived in Eqs. (4.20)-(4.23) of Ref. [21]. From these equations, doing the same calculations as for $B_0(\omega)$, we obtain

$$
\begin{aligned}
B_1(\omega) &= \frac{e^2\hbar\omega_{LO}}{2\epsilon_0(f_{n',0}-f_{n,0})}\frac{1}{2q_d^2} \\
&\times \Big\{|I_{n",n"}|^2\big[(1+N_q)f_{n',0}(1-f_{n",0})-N_qf_{n",0}(1-f_{n',0}) \\
&\quad - (1+N_q)f_{n,0}(1-f_{n",0})+N_qf_{n",0}(1-f_{n,0})\big]\delta(Z_{n',n"}^+) \\
&\times |I_{n",n"}|^2\big[(1+N_q)f_{n",0}(1-f_{n,0})-N_qf_{n,0}(1-f_{n",0}) \\
&\quad - (1+N_q)f_{n",0}(1-f_{n',0})-N_qf_{n',0}(1-f_{n",0})\big]\delta(Z_{n',n"}^-) \\
&- |I_{n',n"}|^2\big[(1+N_q)f_{n',0}(1-f_{n",0})-N_qf_{n",0}(1-f_{n',0})\big]\delta(Z_{n,n"}^-) \\
&+ |I_{n',n"}|^2\big[(1+N_q)f_{n",0}(1-f_{n',0})-N_qf_{n',0}(1-f_{n",0})\big]\delta(Z_{n,n"}^+)\Big\},
\end{aligned}
\tag{11}
$$

and

$$
\begin{aligned}
B_2(\omega) &= \frac{e^2\hbar\omega_{LO}}{2\epsilon_0(f_{n',0}-f_{n,0})}\frac{1}{2q_d^2} \\
&\times \Big\{|I_{n",n"}|^2\big[(1+N_q)f_{n",0}(1-f_{n,0})-N_qf_{n,0}(1-f_{n",0}) \\
&\quad - (1+N_q)f_{n",0}(1-f_{n',0})+N_qf_{n',0}(1-f_{n",0})\big]\delta(Z_{n,n"}^+) \\
&\times |I_{n",n"}|^2\big[(1+N_q)f_{n',0}(1-f_{n",0})-N_qf_{n",0}(1-f_{n',0}) \\
&\quad - (1+N_q)f_{n,0}(1-f_{n",0})-N_qf_{n",0}(1-f_{n,0})\big]\delta(Z_{n,n"}^-) \\
&- |I_{n,n"}|^2\big[(1+N_q)f_{n',0}(1-f_{n",0})-N_qf_{n",0}(1-f_{n',0})\big]\delta(Z_{n',n"}^+) \\
&+ |I_{n,n"}|^2\big[(1+N_q)f_{n",0}(1-f_{n',0})-N_qf_{n',0}(1-f_{n",0})\big]\delta(Z_{n',n"}^-)\Big\},
\end{aligned}
\tag{12}
$$

where we have denoted

$$Z_{n,n'}^{\pm} = 2\hbar\omega - (E_n - E_{n'}) \pm \hbar\omega_{LO}. \tag{13}$$

Inserting Eqs. (9), (11) and (12) into Eqs. (5) and (6), we obtain the analytic expression of linear ($\mathrm{Re}\{\sigma_{zz}(\omega)\}$) and nonlinear term ($\mathrm{Re}\{\sigma_{zzz}(\omega)\}$) of conductivity tensor. We can see that, $\mathrm{Re}\{\sigma_{zzz}(\omega)\}$ includes two photon process. Finally, inserting Eqs. (5) and (6) into Eq. (4), we obtain the real part of the nonlinear conductivity tensor $\mathrm{Re}\{\sigma_{NLn}(\omega)\}$. We have obtained an expression for the absorption power in DSSL, however, delta functions in the expression for $B_0(\omega)$, $B_1(\omega)$ and $B_2(\omega)$ results in the divergence of $B_i(\omega)$ when $Y_{n,n'}^{\pm} = 0$ or $Z_{n,n'}^{\pm} = 0$. To avoid this we replace the delta functions by Lorentzians [32]

$$\delta(Y_{n,n'}^{\pm}) = \frac{1}{\pi} \frac{\hbar\gamma_{n,n'}^{\pm}}{(Y_{n,n'}^{\pm})^2 + \hbar^2(\gamma_{n,n'}^{\pm})^2} \tag{14}$$

where $\gamma_{n,n'}^{\pm}$ is the inverse relaxation time. Using Eq. (A6) from Ref. [32], we have

$$(\gamma_{n,n'}^{\pm})^2 = \frac{1}{\hbar^2}\left(N_q + \frac{1}{2} \pm \frac{1}{2}\right)\frac{e^2\hbar\omega_{LO}}{2\pi\epsilon_0\Omega}\left(\frac{1}{\chi_\infty} - \frac{1}{\chi_0}\right)\frac{1}{2q_d^2}|M_{n,n'}|^2. \tag{15}$$

We can see that these analytical results appear very involved. However, physical conclusions can be drawn from graphical representations and numerical results, obtained by adequate computational methods.

III. NUMERICAL RESULTS AND DISCUSSIONS

It is clearly seen from Eqs. (11) and (12) that $B_1(\omega)$ and $B_2(\omega)$ diverge whenever the arguments in the Delta functions equal to zero. From these conditions, we have

$$2\hbar\omega \pm (n - n')\hbar\omega_p \pm \hbar\omega_{LO} = 0. \tag{16}$$

The Eq. (16) is the NODEPR condition in DSSL. When the NODEPR conditions are satisfied, in the course of scattering events, the electrons in the state $|n\rangle$ could make transitions to one of the other state $|n'\rangle$ by absorbing two photon of energy $\hbar\omega$ during the absorption and/or emitting of a LO phonon of energy $\hbar\omega_{LO}$. In the absence of incident photon ($\omega \to 0$), Eq. (16) reduces to

$$(n - n')\hbar\omega_p = \hbar\omega_{LO}. \tag{17}$$

This is the electrophonon resonance (EPR) condition [33, 34] in DSSL. We can see that, EPR is the specific case of ODEPR in the absence of incident photon.

In clarify the obtained results we numerically calculate the nonlinear absorption power $P_{NLn}(\omega)$ for a DSSL. The nonlinear absorption power is considered as a function of the photon energy. For our numerical results, we use the n-i-p-i superlattice of GaAs:Si/GaAs:Be with the parameters [27, 28, 35, 36]: $m^* = 0.067m_0$ with m_0 being the electron rest mass, a LO-phonon energy $\hbar\omega_{LO} = 36.25$ meV, $s_0 = 100$, $E_0 = 10^5$ V/m; $n = 0, n' = 1$, $n'' = 0$ and 1.

Figure 1 describes the dependence of nonlinear absorption power on the photon energy at $n_D = 10^{23}$ m^{-3}, correspond to $\Delta E_{1,0} = (1 - 0)\hbar\omega_p = 161.32$ meV. From the figure, we can see six peaks, each of ones satisfies a different transition. Three peaks
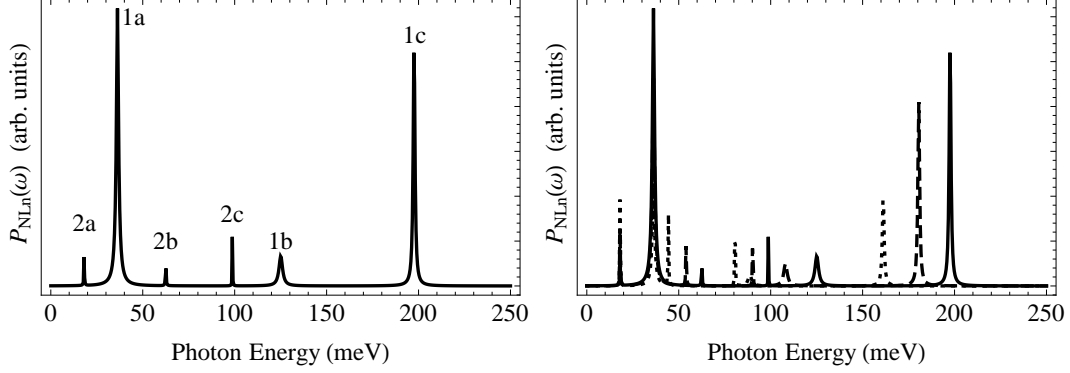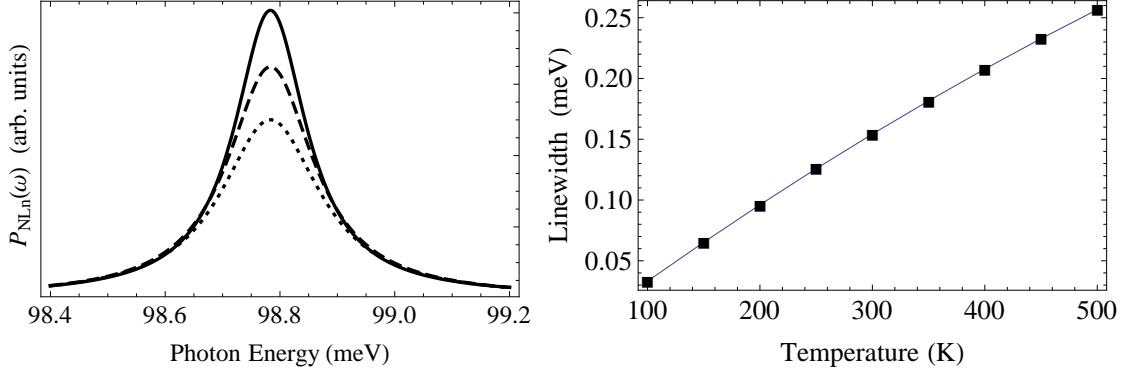
Fig. 1. Left: Nonlinear absorption power $P_{NLn}(\omega)$ as function of photon energy at $T = 300$ K, $d = 20$ nm, $n_D = 10^{23}$ m^{-3}.

Fig. 2. Right: Nonlinear absorption power $P_{NLn}(\omega)$ as a function of the photon energy with different values of the concentration of the donor impurities n_D. The solid, dashed, and dotted lines are for $n_D = 10^{23}$ m^{-3}, 0.8×10^{23} m^{-3}, and 0.6×10^{23} m^{-3}, respectively. Here, $T = 300$ K, d=20 nm.

1a, 1b and 1c correspond to the values $\hbar\omega = 36.25$ meV, 125.07 meV and 197.57 meV, respectively, describe the transitions of electron due to the distribution of one photon absorption process. Three peaks 2a, 2b and 2c correspond to the values $\hbar\omega = 18.13$ meV, 62.53 meV and 98.78 meV, respectively. These peaks describe the transitions of electron due to the distribution of two photon absorption process. We make these peaks clear as follow: The peaks 2a satisfies the condition $2\hbar\omega = \hbar\omega_{LO}$. Therefor, this peak describes intraband transition. Two peaks 2b and 2c satisfy the NODEPR conditions $2\hbar\omega^{\pm} = \Delta E_{1,0} \pm \hbar\omega_{LO}$ or $2\hbar\omega^{\pm} = 161.32 \pm 36.25$ meV, and the distance between two peaks is twice the LO-phonon energy.

   Figure 2 describes the dependence of $P_{NLn}(\omega)$ on the photon energy with different values of the concentration of the donor impurities n_D. From Eq. (3), because $\Delta E_{n,n'} = (n-n')\hbar\omega_p$, with $\omega_p = \sqrt{\frac{4\pi e^2 n_D}{\epsilon_0 m^*}}$, decreases with n_D decreasing. So that, when n_D decreases the resonant peaks shifts to the left (the small region of photon energy). This is because of the decreasing of $\Delta E_{n,n'}$ when the concentration of the donor impurities n_D decreases, consequently, the photon energy that satisfies the ODEPR condition decreases. In the following, we use peak 2c to investigate NODEPR linewidth in DSSL.
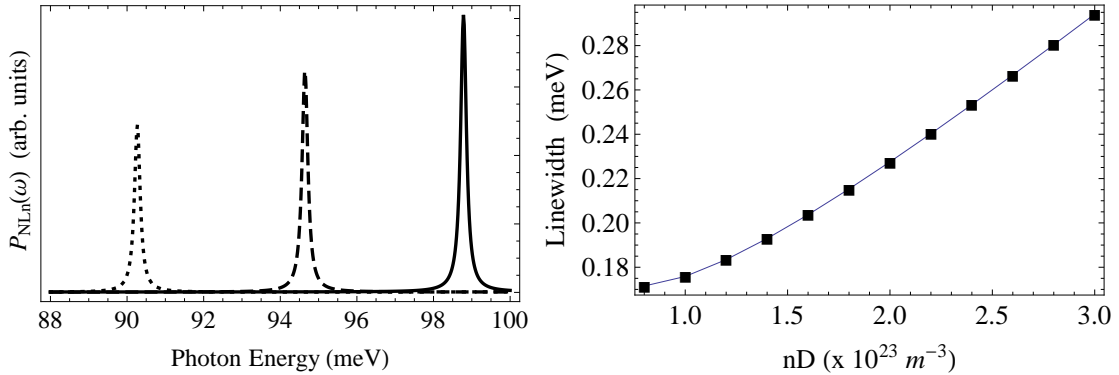
   Figure 3 describes the dependence of $P_{NLn}(\omega)$ on the photon energy with different values of temperature T at $d = 20$ nm, $n_D = 10^{23}$ m^{-3}, corresponds to $\Delta E_{1,0} = 161.32$ meV. From the figure we can see that, all peaks locate at the same position $\hbar\omega = 98.78$ meV, corresponding to the NODEPR condition $2\hbar\omega = \Delta E_{1,0} + \hbar\omega_{LO} = 161.32 + 36.25$ meV, and is independent of T. From these curves, using profile method presented in our previous paper [19], we obtain the temperature dependence of the NODEPR linewidth' as shown in Fig. 4.

Fig. 3. Left: Nonlinear absorption power $P_{NLn}(\omega)$ as a function of the photon energy with different values of temperature T. The solid, dashed, and dotted lines are for $T = 250$ K, 300 K, and 350 K, respectively. Here, $d = 20$ nm, $n_D = 10^{23}$ m^{-3}.

Fig. 4. Right: Dependence of NODEPR linewidth on temperature T at $d = 20$ nm, $n_D = 10^{23}$ m^{-3}.

Figure 4 shows that the NODEPR linewidth increases with temperature T. This behavior is in agreement with linear theoretical results of Kang *et al.* [2], Li and Ning [4] and experimental results of Unuma *et al.* [12] in quantum well. Because, as temperature increases, the probability of electron-phonon scattering increases, so that NODEPR linewidth rises.
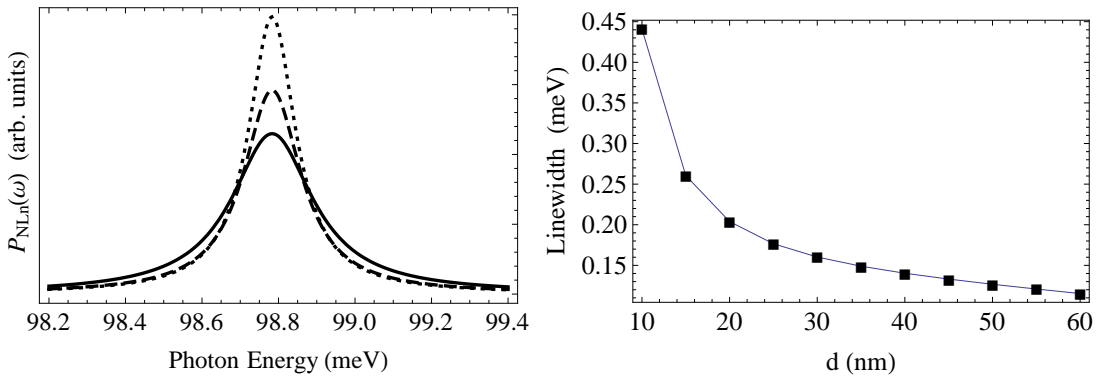

Fig. 5. Left: Nonlinear absorption power $P_{NLn}(\omega)$ as a function of the photon energy with different values of the concentration of the donor impurities n_D. The solid, dashed, and dotted lines are for $n_D = 10^{23}$ m^{-3}, 0.9×10^{23} m^{-3}, and 0.8×10^{23} m^{-3}, respectively. Here, $T = 300$ K, $d = 20$ nm.

Fig. 6. Right: Dependence of NODEPR linewidth on the concentration of the donor impurities n_D at $T = 300$ K, $d = 20$ nm.

Figure 5 describes the dependence of $P_{NLn}(\omega)$ on the photon energy with different values of the concentration of the donor impurities n_D. The figure shows that, the maxima appear at the photon value of $\hbar\omega = 98.78$ meV, 94.64 meV, and 90.27 meV for $n_D = 10^{23}$ m^{-3}, 0.9×10^{23} m^{-3}, and 0.8×10^{23} m^{-3}, respectively. As the concentration of the donor impurities n_D decreases, the peak position is shifted to the lower photon energy region. Because, when the n_D decreases, $\Delta E_{1,0}$ decreases, so the values of photon energy absorbed, which correspond to the NODEPR condition $2\hbar\omega = \Delta E_{1,0} + \hbar\omega_{LO}$ decreases. From the figure, we obtain the concentration of the donor impurities dependence of the NODEPR linewidth's as shown in Fig. 6.

Figure 6 shows that, NODEPR linewidth increases with n_D. This can be explained that as n_D increases, the plasma frequency ω_p increases, the radius $\ell_p = \sqrt{\hbar/(m*\omega_p)}$ reduces, the confinement of electron increases, the probability of electron-phonon scattering increases, so that linewidth rises.

Fig. 7. Left: Nonlinear absorption power $P_{NLn}(\omega)$ as a function of the photon energy with different values of the periods of the DSSL d. The solid, dashed, and dotted lines are for $d = 10$ nm, 20 nm and 30 nm, respectively. Here, $T = 300$ K, $n_D = 10^{23}$ m^{-3}.

Fig. 8. Right: Dependence of NODEPR linewidth on the periods of the DSSL d at $T = 300$ K, $n_D = 10^{23}$ m^{-3}.

Figure 7 describes the dependence of $P_{NLn}(\omega)$ on the photon energy with different values of d at $T = 300$ K, $n_D = 10^{23}$ m^{-3}, corresponds to $\Delta E_{1,0} = 161.32$ meV. From the figure we can see that, all peaks locate at the same position $\hbar\omega = 98.78$ meV, corresponding to the NODEPR condition $2\hbar\omega = \Delta E_{1,0} + \hbar\omega_{LO} = 161.32 + 36.25$ meV, and is independent of d. From these curves we obtain the periods of the DSSL dependence of the NODEPR linewidth' as shown in Fig. 8.

Figure 8 shows that, NODEPR linewidth decreases with the periods of the DSSL d. This result is in agreement with theoretical results of Unuma *et al.* [1], and Kang's results [2] in quantum well. All of them show the decreasing of linewidth with system's size increasing. This can be explained that as the wire's radius increases the confinement of electron decreases, the probability of electron-phonon scattering decreases, so

that NODEPR linewidth drops. However, the value of nonlinear linewidth in our result is smaller than linear ones. It means that, the distribution of two photon absorption process is smaller than one photon absorption process ones.

IV. CONCLUSION

So far, we have obtained analytic expression of nonlinear absorption power in DSSL due to electron-LO-phonon interaction. We numerically calculated and plotted $P_{NLn}(\omega)$ for the n-i-p-i superlattice of GaAs:Si/GaAs:Be to clarify the theoretical results, and obtained the NODEPR conditions.

Special attention is given to the behavior of the NODEPR spectrum, such as the splitting of NODEPR peaks due to the selection rules. The peak splitting are satisfied the NODEPR condition $2\hbar\omega \pm (n - n')\hbar\omega_p \pm \hbar\omega_{LO} = 0$. As n_D increases, the resonant peaks shift to the small region of photon energy, but the distance between two NODEPR peaks is always twice as much as the LO-phonon energy.

From the graphs of the nonlinear absorption power, we obtained NODEPR linewidth as profiles of curves. Computational results show that the NODEPR linewidth increases with temperature and concentration of the donor impurities, and decreases with periods of the DSSL. The contribution of two photons absorption process to absorption power is smaller than ones of one photon process. The results are clear in physical interpretation, and agree with some previous results.

ACKNOWLEDGMENT

REFERENCES

[1] T. Unuma, M. Yoshita, H. Noda, H. Sakaki, H. Akiyama, *J. Appl. Phys.* **93** (2003) 1586.

[2] N. L. Kang, S. D. Choi, *J. Phys.: Condens. Matter* **14** (2002) 9733.

[3] N. L. Kang, D. H. Shin, S. N. Yi, S. D. Choi, *J. Kor. Phys. Soc.* **46** (2005) 1040.

[4] J. Li, C. N. Ning, *Phys. Rev. B* **70** (2004) 125309.

[5] H. C. Chui, E. L. Martinet, M. M. Fejer, J. S. Harris, *Appl. Phys. Lett.* **64** (1994)736.

[6] Y. Arakawa, K. Vahala, A. Yariv, K. Lau, *Appl. Phys. Lett.* **48** (1986) 384.

[7] H. Ham, H. N. Spector, *Phys. Rev. B* **62** (2000) 13599.

[8] H. Ham, H. N. Spector, *J. Appl. Phys.* **90** (2001) 2781.

[9] H. Weman, L. Sirigu, K. F. Karlsson, K. Leifer, A. Rudra, E. Kapon, *Appl. Phys. Lett.* **81** (2002) 2839.

[10] M. Abul Khayer, A. Haque, *J. Appl. Phys.* **100** (2006) 113108.

[11] N. Yamamoto, K. Akahane, T. Kawanishi, Y. Omigawa, H. Sotobayashi, Y. Yoshioka, H. Takai, *Opt. Express* **19**(2011) B636.

[12] T. Unuma, T. Takahashi, T. Noda, M. Yoshita, H. Sasaki, M. Baba, H. Akiyama, *Appl. Phys. Lett.* **78** (2001) 3448.

[13] V. V. Bryksin, Yu. A. Firsov, S. A. Ktitorov, *Solid State Commun.* **39** (1981) 385.

[14] M. V. Kisin, M. A. Stroscio, G. Belenky, S. Luryi, *Appl. Phys. Lett.* **80** (2002) 2174.

[15] S. C. Lee, J. W. Kang, H. S. Ahn, M. Yang, N. L. Kang, S. W. Kim, *Physica E* **28** (2005) 402.

[16] S. G. Yu, V. B. Pevzner, and K. W. Kim, M. A. Stroscio, *Phys. Rev. B* **58** (1998) 3580.

[17] S. C. Lee, *J. Kor. Phys. Soc.* **52** (2008) 1832.

[18] S. C. Lee, *J. Kor. Phys. Soc.* **52** (2008) 1801.

[19] T. C. Phong, H.V. Phuc, *Mod. Phys. Lett. B* **25** (2011) 1003.

[20] T. C. Phong, L. T. T. Phuong, L. Dinh, H. V. Phuc, *Proc. Natl. Conf. Theor. Phys.* **35** (2010) 135.

[21] H. J. Lee, N. L. Kang, J. Y. Sug, S. D. Choi, *Phys. Rev. B* **65** (2002) 195113.

[22] D. Dunn, A. Suzuki, *Phys. Rev. B* **29** (1984) 942.

[23] Y. J. Cho, S. D. Choi, *Phys. Rev. B* **49** (1994) 14301.

[24] T. C. Phong, L. V. Tung, N. Q. Bau, *J. Kor. Phys. Soc.* **53** (2008)1971.

[25] N. L. Kang, Y. J. Lee, S. D. Choi, *J. Kor. Phys. Soc.* **44** (2004) 1535.

[26] V. V. Pavlovic, E. M. Epstein, *Sol. Stat. Phys.* **19** (1977) 1760.

[27] A. P. Silin, *Sov. Phys. Usp.* **28** (1986) 972.

[28] K. Ploog, G. H. Dohler, *Adv. Phys.* **32** (1983) 285.

[29] G. M. Shmelev, I. A. Chaikovskii, V. V. Pavlovich, E. M. Epshtein, *Phys. Stat. Sol.* (b) **80** (1977) 697.

[30] S. N. Yi, J. J. Song, K. S. Bae, S. D. Choi, *Physica B* **222** (1996) 209.

[31] N. L. Kang, S. D. Choi, *J. Phys. Soc, Jpn.* **78** (2009) 024710.

[32] M.P. Chaubey, C.M.V. Vliet, *Phys. Rev. B* **33** (1986) 5617.

[33] K. L. Ngai, E. N. Economou, J. Ruvalds, *Phys. Rev. B* **6** (1972) 2506.

[34] W. Xu, F. M. Peeters, J. T. Devreese, *J. Phys.: Condens Matter* **5**, (1993) 2307.

[35] Y. He, Z. Yin, M. S. Zhang, T. Lu and Y. Zheng, *Mat. Sci. Eng. B* **75** (2000) 130.

[36] N. Mori, H. Momose and C. Hamaguchi, *Phys. Rev. B* **45** (1992) 4536.